bioRxiv preprint doi: https://doi.org/10.1101/2021.07.19.452678; this version posted July 19, 2021. The copyright holder for this preprint (which was not certified by peer review) is the author/funder, who has granted bioRxiv a license to display the preprint in perpetuity. It is made available under aCC-BY 4.0 International license.

The amplitude of fNIRS hemodynamic response in the visual cortex unmasks autistic traits in typically developing children

Raffaele Mazziotti[1,2‡], Elena Scaffei[2,3‡], Eugenia Conti[3], Viviana Marchi[3], Riccardo Rizzi[2,3], Giovanni Cioni[3,4], Roberta Battini[3,4], Laura Baroncelli[1,3*]

[1] Institute of Neuroscience, National Research Council (CNR), I-56124, Pisa, Italy
[2] Department of Neuroscience, Psychology, Drug Research and Child Health NEUROFARBA, University of Florence, I-50135, Florence, Italy
[3] Department of Developmental Neuroscience, IRCCS Stella Maris Foundation, I-56128, Pisa, Italy
[4] Department of Clinical and Experimental Medicine, University of Pisa, Pisa, Italy

*To whom correspondence should be addressed: baroncelli@in.cnr.it
‡These authors equally contributed to the work

bioRxiv preprint doi: https://doi.org/10.1101/2021.07.19.452678; this version posted July 19, 2021. The copyright holder for this preprint (which was not certified by peer review) is the author/funder, who has granted bioRxiv a license to display the preprint in perpetuity. It is made available under aCC-BY 4.0 International license.

Abstract

Autistic traits represent a continuum dimension across the population, with autism spectrum disorder (ASD) being the extreme end of the distribution. Accumulating evidence shows that neuroanatomical and neurofunctional profiles described in relatives of ASD individuals reflect an intermediate neurobiological pattern between the clinical population and healthy controls. This suggests that quantitative measures detecting autistic traits in the general population represent potential candidates for the development of biomarkers identifying early pathophysiological processes associated with ASD. Functional near-infrared spectroscopy (fNIRS) has been extensively employed to investigate neural development and function. In contrast, the potential of fNIRS to define reliable biomarkers of brain activity has been barely explored. Features of non-invasiveness, portability, ease of administration and low-operating costs make fNIRS a suitable instrument to assess brain function for differential diagnosis, follow-up, analysis of treatment outcomes and personalized medicine in several neurological conditions. Here, we introduce a novel standardized procedure with high entertaining value to measure hemodynamic responses (HDR) in the occipital cortex of adult subjects and children. We found that the variability of evoked HDR correlates with the autistic traits of children, assessed by the Autism-Spectrum Quotient. Interestingly, HDR amplitude was especially linked to social and communication features, representing the core symptoms of ASD. These findings establish a quick and easy strategy for measuring visually-evoked cortical activity with fNIRS that optimize the compliance of young subjects, setting the background for testing the diagnostic value of fNIRS visual measurements in the ASD clinical population.

bioRxiv preprint doi: https://doi.org/10.1101/2021.07.19.452678; this version posted July 19, 2021. The copyright holder for this preprint (which was not certified by peer review) is the author/funder, who has granted bioRxiv a license to display the preprint in perpetuity. It is made available under aCC-BY 4.0 International license.

Introduction

Autism spectrum disorder (ASD) is a heterogeneous developmental condition that involves persistent challenges in social interactions, restricted/repetitive behaviors, and the lack of behavioral and cognitive flexibility[1]. Since the pioneering work by Lorna Wing[2], increasing epidemiological evidence indicates that autistic traits are continuously distributed across the general population[3,4]. This is due to the complex genetic and epigenetic inheritance pattern of ASD, where multiple candidate loci contribute to the pathogenesis of the disease[5,6]. Milder autistic traits have been termed the extended or broader autism phenotype (BAP), with BAP features being particularly prevalent in first- and second-degree relatives of individuals with ASD[6–9]. Since ASD and broader autistic manifestations share common genetic variants and neurobiological susceptibility factors[10], the general population emerges as a suitable testing bed for the development of quantitative measures detecting neurostructural and neurofunctional hallmarks of autism.

Over the last decade, the biological dimension of ASD has been largely explored, thanks to the growing availability of advanced tools to explore brain correlates of neurological disorders, including high-density EEG, magnetoencephalography, positron emission tomography, magnetic resonance imaging (MRI), and functional near-infrared spectroscopy (fNIRS)[8,11,12]. A number of studies reported defective neuroanatomical and neurofunctional features in individuals with ASD, suggesting that a dysfunction of specific brain areas might underlie the core symptoms of ASD[13–17]. Interestingly, similar neurological profiles describe the relatives of autistic probands[8].

FNIRS is an optical imaging technique that allows quantifying oxygen consumption in different regions of the cerebral cortex, providing an indirect measure of neuronal activity[18,19]. This blood-oxygen-level-dependent (BOLD) signal is similar to that detected with functional MRI (fMRI)[20]. However, fNIRS is more tolerant to motion artifacts than fMRI, and the development of robust methods for motion detection and correction allowed to avoid sedation in children[21,22]. Furthermore, fNIRS has the advantage of being totally non-invasive, low-cost, portable, noiseless, and endowed with high experimental flexibility and no setting constraints. This methodological strength provides the fNIRS with a high ecological value for investigating neural circuit maturation either in typically developing children or clinically relevant populations[21,23].

bioRxiv preprint doi: https://doi.org/10.1101/2021.07.19.452678; this version posted July 19, 2021. The copyright holder for this preprint (which was not certified by peer review) is the author/funder, who has granted bioRxiv a license to display the preprint in perpetuity. It is made available under aCC-BY 4.0 International license.

Although the use of fNIRS in autism research is still an emerging area, a number of studies aiming to decipher the neuronal mechanisms and circuits underlying ASD evaluated different aspects of brain function and organization, including resting-state and task-evoked responses[24,25]. Coherence analyses of resting-state hemodynamic activity showed weaker local and interhemispheric functional connectivity in different cortical regions[26–31]. Moreover, individuals on the autism spectrum present patterns of atypical activity, including reduced hemodynamic responses within specific brain regions, bilateral differences in neuronal activation and the lack of cortical specialization, in tasks ranging from sensory perception[32] to executive functions[33], social perception[34–37], joint attention[38–40], imitation[41,42], facial and emotional processing[43–46], speech perception and language[47–50]. The majority of studies targeting evoked brain activity was focused on the prefrontal and the temporal cortex[25], where symptom severity seems to be inversely correlated with the degree of cortical activation[42,43].

Growing evidence suggests that fNIRS might be a candidate biomarker for several neuropsychiatric disorders, including ASD[29,51–55]. In particular, functional network efficiency[29], weighted separability of NIRS signals[56], multi-layer neural networks and sample entropy of spontaneous hemodynamic fluctuations[54,57] have been proposed as auxiliary diagnosis indexes for ASD. However, all these approaches require complex algorithms to extract high-level features from the fNIRS raw data, while fitness, applicability and translational value of biomarkers greatly depend on their ease of use. In this framework, the analysis of visual phenotype has become an important model to evaluate cortical processing in different neurodevelopmental conditions[58–63]. Indeed, electrophysiological measurement of visually evoked responses has been introduced as a quantitative method to assess brain function in Rett syndrome[58,64], and hemodynamic responses (HDR) emerged as a potential longitudinal biomarker for CDKL5 Deficiency Disorder and Creatine Transporter Deficiency in murine models[62,63].

Since clinical studies suggested a dysregulation of sensory processing and functional connectivity in the visual cortex of ASD subjects[65–67], we hypothesized that fNIRS visual measures could be related to broad autism dimensions in the general population. To address this issue, we developed a novel standardized procedure to assess HDR changes in the occipital cortex testing 40 randomly selected neuro-

bioRxiv preprint doi: https://doi.org/10.1101/2021.07.19.452678; this version posted July 19, 2021. The copyright holder for this preprint (which was not certified by peer review) is the author/funder, who has granted bioRxiv a license to display the preprint in perpetuity. It is made available under aCC-BY 4.0 International license.

typical adults and 19 children, and measuring inter-individual differences in autistic traits, using the Autism-Spectrum Quotient (AQ[68,69]).

Results

An animated cartoon-based stimulus is able to evoke visual responses in the adult cortex

We measured the cortical HDR function[70] elicited by a reversing checkerboard pattern in the adult population. In agreement with the previous literature[71,72], we obtained a significant activation of the occipital cortex in response to different conditions of visual stimulation (Fig. 1 and Fig. S1). Grand averages across adult participants (see Table 1 for demographics) of Total Hb (THb), OxyHb (OHb) and DeoxyHb (DHb) concentration changes are plotted in Fig. 2. Using a classic mean-luminance grey screen as baseline, statistical analysis revealed a significant main effect of the checkerboard stimulus (S) with respect to the blank presentation for all HDR metrics (Radial Stimulus condition, RS, Fig. 2A).

To increase the entertaining quality of our experimental paradigm, we devised an innovative visual stimulation protocol blending the checkerboard pattern with an isoluminant commercial cartoon, thus serving as a reference baseline (Fig. 1 and Fig. S1). We found a significant increase of THb and OHb, with a parallel reduction of DHb concentration, in response to S appearance, reflecting the functional activation of visual areas in this condition as well. The cortical response was independent from the cartoon employed as baseline: a comparable HDR, indeed, was clearly elicited both when the baseline movie was fixed a priori by the experimenter (Cartoon Fixed condition, CF; Fig. 2B) and when the cartoon was freely selected by the tested subject (Cartoon Chosen condition, CC; Fig. 2C). Interestingly, a significant pattern of correlations emerged among HDR metrics recorded with different stimulating conditions (Fig. S2), indicating that the quality of visual input does not quantitatively impact HDR. The amplitude of cortical activation was only slightly smaller in response to CF and CC, with the range of OHb and DHb fluctuations being significantly lower with respect to that evoked by RS (Fig. 2D).

Within the CF condition, we also established that the baseline cartoon does not affect the degree of visual activation: indeed, a comparable modification of THb, OHb and DHb concentrations was recorded using “The Lion King”, “The Powerpuff Girls”, “Peppa Pig” or “Kung Fu Panda” (Fig. S3A). Furthermore, no differences of

bioRxiv preprint doi: https://doi.org/10.1101/2021.07.19.452678; this version posted July 19, 2021. The copyright holder for this preprint (which was not certified by peer review) is the author/funder, who has granted bioRxiv a license to display the preprint in perpetuity. It is made available under aCC-BY 4.0 International license.

visually evoked responses were detected modulating the contrast level of the baseline cartoon: THb, OHb and DHb fluctuations, indeed, were comparable when a fixed baseline cartoon was presented at 20%, 40%, or 80% of contrast (Fig. 2E; Fig. S3B-D). Finally, the response latency was homogenous in RS, CF, and CC conditions (Fig. S4A).

Altogether, these results demonstrate the validity of this innovative stimulation procedure to evoke a significant and reliable response in the occipital cortex preserving inter-subject variability.

The cartoon paradigm was reliable in eliciting cortical responses in children

We measured cortical responses in typically developing children (see Table 2 for demographics) viewing the radial checkerboard blended with the animated cartoon. We compared three different conditions: each subject, indeed, was asked to select two cartoons of their preference for the baseline and the first choice was employed for the low-contrast (cartoon 1 low contrast, 20%, L1) and the high-contrast (cartoon 1 high contrast, 80%, H1) stimulation, while the second cartoon was presented only at low-contrast (cartoon 2 low contrast, L2; Fig. S1).

Our data showed a significant activation of the visual cortex, with a prominent change of THb, OHb and DHb concentration in response to the S with respect to the blank for all conditions tested (Fig. 3A-C). The amplitude of elicited cortical responses was comparable following L1, H1 and L2 (Fig. 3D), proving that the HDR is independent from the cartoon narrative selected for the baseline and the contrast level of baseline presentation in children as well. Small differences were observed for response latency among L1, H1 and L2 conditions (Fig. S4B). A highly significant pattern of correlations among different HDR indexes recorded in the diverse conditions was detected (Fig. S5).

In agreement with previous literature[72], a maturational trend of cortical responsivity was recognized, with children showing significantly higher HDR amplitude with respect to adult subjects (Fig. 3E). On the contrary, age-dependent effects were not identified for response latency (Fig. S4C).

These findings establish a novel method for measuring visually-evoked cortical activity with fNIRS that ensures an elevated compliance of young subjects and high-quality reliability of measurements, suggesting a valuable tool for studying

bioRxiv preprint doi: https://doi.org/10.1101/2021.07.19.452678; this version posted July 19, 2021. The copyright holder for this preprint (which was not certified by peer review) is the author/funder, who has granted bioRxiv a license to display the preprint in perpetuity. It is made available under aCC-BY 4.0 International license.

visual cortical processing in typically developing children, but also in clinically relevant populations.

Negative correlation of HDR amplitude with AQ score

Despite no effects detectable in adults (Fig. 4A-C), the amplitude of visual responses was highly correlated to AQ scores in children (Fig. 4D-E). Consistent with a recent work[54], the correlation was specific for THb, with higher AQ score being associated with a lower amplitude of THb visually-evoked signals (Fig. 4D-E).

Interestingly, HDR amplitude was especially linked to social and communication autistic traits (Fig. 5, S6): indeed, assessing separately the five AQ subscales[69] we found a significant correlation of THb and OHb with the Social Skills subscale (AQ_S, Fig. 5A-B), while only THb modulation was related to the Communication subscale (AQ_C, Fig. 5C-D). Given the reliability across different visual tasks (L1 and H1), the strongest interaction was between THb and AQ_S (Fig. 5A-B).

Discussion

We measured hemodynamic responses in the occipital cortex while subjects viewed a reversing checkerboard pattern on a grey isoluminant baseline or the same stimulus blended with a commercial animated cartoon. In all participants, the patterned stimulus elicited a significant change of cortical Hb (upwards for THb and OHb, down for DHb) independently from the reference baseline, while no response was detected following blank presentation. Since HDR consists of an initial increase in oxygen rich blood followed by a smaller depletion of deoxy-haemoglobin, with a tight interrelation among total, oxygenated and reduced Hb levels, reporting all data allows for a more accurate physiological interpretation of the results[70].

Interestingly, the level of occipital cortex activation did not depend on either the movie selected as reference baseline or the baseline contrast, with only a slight reduction of OHb and DHb change in response to the stimulus blended to animated cartoons with respect to the classic RS condition. These data demonstrate the reliability of this novel procedure with high entertaining and ecological value in eliciting cortical activity. Thus, our approach might be helpful for studying cortical function in children with an atypical trajectory of brain development, commonly showing a reduced compliance in experimental environments.

bioRxiv preprint doi: https://doi.org/10.1101/2021.07.19.452678; this version posted July 19, 2021. The copyright holder for this preprint (which was not certified by peer review) is the author/funder, who has granted bioRxiv a license to display the preprint in perpetuity. It is made available under aCC-BY 4.0 International license.

The magnitude of HDR modulation, and in particular of THb, was inversely correlated with AQ scores in children. Indeed, we found that the higher were the AQ scores of subjects the lower was the amplitude of THb response to visual stimulation, suggesting that visually-evoked fNIRS responses are able to capture the dimension of autistic traits in the general young population. Our findings are consistent with previous studies showing that cortical activation measured with fNIRS and the performance in visual psycophysics negatively reflected ASD symptom severity[42,43,73–76]. Moreover, these data reinforce the concept that THb changes could provide richer discriminative information for classifying between typically developing children and ASD subjects[54]. A tentative explanation of reduced HDR in children with stronger autistic traits might be found in the difference of perceptual styles in the general population[77,78]: the preference for focusing on local details vs. the global stimulus configuration, indeed, is a defining feature of ASD[79] and locally centered perception could be less effective in activating neural circuits of visual cortex. Interestingly, a recent study established a vascular link to ASD, showing early dysfunction of endothelial cells and impaired endothelium-dependent vasodilation in a mouse model of 16p11.2 deletion[80]. Since the HDR measured with fNIRS strongly relies on neurovascular coupling, this suggests that lower neurophysiological activity may stem in part from endothelial-dependent vascular factors. In contrast, we failed to detect any correlation between HDR and AQ scores in adult subjects. This is likely due to the different dynamic range and amplitude of HDR responses measured in children and adult participants. Accordingly, the maturation of neural and vascular networks over the first years of life affects neurovascular coupling with a pattern of hemodynamic responses significantly different in developing and adult brain[81].

In our experiment, the THb index describes about 45% of the variance in AQ scores. This correlation is remarkably high, considering that it is detected across two separate visual stimulating procedures, i.e., the vision of low- and the high-contrast blended RS-animated cartoons. Although the autistic questionnaire for children is well-validated, showing good test-retest reliability and high internal consistency, not all items have the same validity and factor analysis identified five subscales, named ‘Social Skills’, ‘Communication’, ‘Attention to Detail’, ‘Imagination’ and ‘Attention Switching’[69]. We observed variability in the strength of correlation between HDR and AQ subscales, with the highest correlation for the ‘Social Skills’ and ‘Communication’

bioRxiv preprint doi: https://doi.org/10.1101/2021.07.19.452678; this version posted July 19, 2021. The copyright holder for this preprint (which was not certified by peer review) is the author/funder, who has granted bioRxiv a license to display the preprint in perpetuity. It is made available under aCC-BY 4.0 International license.

subscales. Interestingly, 'Social Skills' and 'Communication' are the subscales with higher construct validity performance in differentiating individuals with or without ASD[82,83], while 'Attention to Detail' was the poorest classifying domain[84]. It is also worth stressing that among the items composing the 'Attention to Detail' subscale, only four actually relate to sensory perception (e.g. 'My child usually notices details that others do not'), the others being more focused on cognitive functions (e.g. 'My child is fascinated by numbers'). Accordingly, the first pilot report of the AQ questionnaire showed lower internal consistency (measured by Cronbach's alpha coefficient) of 'Attention to Detail' items compared to other subscales[68].

Although primarily affecting social functioning, there is a growing body of evidence showing that ASD is also associated with abnormalities in multiple sensory domains, fluctuating between hyper- and hypo-sensitivity to sensory stimuli[73,85]. In addition to a higher incidence of refractive errors and strabismus[86], anomalies in visual processing, visual attention and visual-motor integration have been described in ASD population[66,73,87]. Interestingly, sensory symptoms are correlated with the severity of the disorder, at least in children[88]. Moreover, commonly observed alterations in social skills might have a visual component[73] and perception deficits could impact with cascading effects on the maturation of cognitive and social domains[87].

It has been recently suggested that an early assessment of pupil size modulation and visual behavior might improve the diagnostic process of ASD[66,77,87,89]. Currently, ASD diagnosis and follow-up almost entirely rely on phenotypic information collected via clinical measures and parental input that are highly prone to subjective bias[90]. Moreover, the late appearance of some behavioral autistic traits often delays the diagnosis until mid-childhood[91,92]. Thus, the identification of solid brain biomarkers early predicting ASD pathophysiology is a critical step to anticipate tailored interventions, leading to better outcomes for patients and possibly even the prevention of certain behaviors typically associated with ASD. Objective biomarkers have also the potential to be helpful in the management of patients, allowing the classification of disease severity and monitoring response to treatments[12]. A recent systematic review highlighted that both functional and structural neuroimaging features might predict ASD diagnosis in the early pre-symptomatic period[93,94], but further studies are needed to validate the promising performance of such biomarkers [12]. Lately, resting-state fNIRS

bioRxiv preprint doi: https://doi.org/10.1101/2021.07.19.452678; this version posted July 19, 2021. The copyright holder for this preprint (which was not certified by peer review) is the author/funder, who has granted bioRxiv a license to display the preprint in perpetuity. It is made available under aCC-BY 4.0 International license.

measurements have been suggested as candidate biomarkers for ASD[29,54,56,57]. As stressed above, fNIRS offers significant advantages with respect to other neuroimaging tools, including non-invasiveness, ease of use, no need of sedation, tolerance to movements and portability, making it a child-friendly approach. However, the extraction of metrics with diagnostic value from resting-state recordings involves complex algorithms.

In contrast, our analysis of visually evoked responses is quick, easy and requires only that children pay attention to a short movie of their choice. Since our stimulating strategy has been studied to optimize the compliance of young subjects, we believe that our results might set the background for testing the predictive value of fNIRS visual measurements to empower early detection of autistic traits. Moreover, screening for autistic traits in the general population may be helpful in epidemiological research because it may provide a large sample size to investigate the correlation between autism phenotype severity and other pathophysiological processes[83].

Materials and methods

Subjects

We recruited a total of 40 adult subjects (20 women, age: 31.05 ± 3.94 (SD) years) and 19 children (5 girls, age: 7.20 ± 3.01 (SD) years). All participants reported normal or corrected-to-normal vision and had no diagnosed neuropsychiatric condition. Experimental procedures on children were authorized by the Regional Pediatrics Ethics Board (Comitato Etico Pediatrico Regionale-Azienda Ospedaliero-Universitaria Meyer-Firenze, Italy; authorization number 201/2019) and were performed according to the declaration of Helsinki. Written informed consent was obtained from all adult participants and from the parents of each child, authorizing the use of anonymized data for research purposes. Assent was also obtained from the children involved in the study before participation.

AQ score

Adult participants filled in the Autistic-traits Quotient (AQ) questionnaire, a 50-items self-administered report validated for the Italian version[68,95]. The items consist of descriptive statements assessing personal preferences and typical behavior. For each item, participants respond on a 4-point Likert scale: ‘‘strongly agree’’, ‘‘slightly

bioRxiv preprint doi: https://doi.org/10.1101/2021.07.19.452678; this version posted July 19, 2021. The copyright holder for this preprint (which was not certified by peer review) is the author/funder, who has granted bioRxiv a license to display the preprint in perpetuity. It is made available under aCC-BY 4.0 International license.

agree'', ''slightly disagree'', and ''strongly disagree''. The items are grouped in five subscales: Social Skills, Communication, Attention to Details, Imagination and Attention Switching. All the questionnaires were scored by a neuropsychiatrist blinded to subject data: 1 point was assigned when the participant's response was characteristic of ASD (slightly or strongly), 0 points were attributed otherwise. Total scores range between 0 and 50, with 32 being the clinical threshold for autism risk[68]. No subjects scoring above 32 points were recorded. The mean (min-max) of the scores was 15.0 (3-32) with SD of 6.5. Since child self-report might be affected by reading and comprehension difficulties, the children's version of Autism Spectrum Quotient (Italian version of AQ-child) was completed by parents[69]. This version of the AQ questionnaire includes 50 items as well, grouped in the same subscales described above, and parents were required to report for each statement the degree of consistency with their child's behavior. Scores range from 0 to 150, since the response scale is treated as a 4-point Likert scale with 0 representing definitely agree; 1 slightly agree; 2 slightly disagree; and 3 definitely disagree. Items were reverse scored as needed. The threshold score is 76[69]. All subjects scored below 76 points. The mean (min-max) of the scores was 32.1 (17-49) with SD of 10.7.

Apparatus and montages

To measure changes in total Hb (THb) concentration and relative oxygenation levels (OHb and DHb) in the occipital cortex during the task, we used a continuous-wave NIRS system (NIRSport 8x8, NIRx Medical Technologies LLC, Berlin, Germany). Our NIRSport system consists of 8 red light-sources operating at 760 nm and 850 nm, and 7 detectors which can be placed into a textile EEG cap (EASYCAP, Herrsching, Germany), forming an array of 22 multi-distant channels[96]. Textile EEG caps of different sizes were used. The probe arrangement was fixed in each of the caps using grommets, optode stabilizers, colored labels and holders in order to assure comparable probe mapping over all subjects. For data recording, the Aurora Software 1.4.1.1 (NIRx Medical Technologies LLC) was employed. The sampling rate was 10.2 Hz. Visual areas were identified according to the craniocerebral topography within the international 10-20 system and the placement of the optodes was done using fOLD v2.2[97] and NIRSite 2.0 (NIRx Medical Technologies LLC) softwares. Sources and detectors were symmetrically distributed to define 22 channels around the region of interest, each adjacent pair of sources and detectors

bioRxiv preprint doi: https://doi.org/10.1101/2021.07.19.452678; this version posted July 19, 2021. The copyright holder for this preprint (which was not certified by peer review) is the author/funder, who has granted bioRxiv a license to display the preprint in perpetuity. It is made available under aCC-BY 4.0 International license.

377 defining one channel (min-max source-detector separation: 20-44 mm for adults, 22-
378 30 mm for children; Fig. S2).
379
380 **Experimental Design and Visual Stimulation**
381 Prior to the experiment, adult participants (or parents for children) filled in the AQ
382 questionnaire. Then, subjects were asked to sit on a comfortable chair and the fNIRS
383 cap was positioned. Optodes were placed into the cap and the calibration of light
384 coupling between sensors and detectors was performed. All experimental sessions
385 lasted 30 minutes. Visual stimuli were generated using Python 3 and Psychopy3 [98]
386 and displayed with gamma correction on a monitor (Sharp LC-32LE352EWH, 60Hz
387 refresh rate, 45 cd/m^2 mean luminance, resolution of 800×600 pixels) placed 70 cm
388 from the subject. Cortical hemodynamics in response to full-field, reversing, square
389 wave, radial checkerboard, with abrupt phase inversion (spatial frequency: 0.33
390 cycles per degree, temporal frequency: 4 Hz; Fig. 1A) was evaluated in the time
391 domain by measuring the peak-to-baseline amplitude and latency. To have an
392 internal control with blank stimulation, we used an event-related design consisting of:
393 i) 20 cycles of 5 seconds stimulus 'on' (reversing checkerboard, 90% of contrast)
394 followed by 10 seconds stimulus 'off' and ii) 20 cycles of 5 seconds mock stimulus
395 'on' (reversing checkerboard, 0% of contrast) followed by 10 seconds stimulus 'off'.
396 The two stimulating conditions were pseudo randomly interleaved for each subject
397 during the recording. Blocks lasted 10 minutes and participants were permitted to
398 take rest between recordings. Fig. 1D shows a schematic representation of the
399 experimental procedure. Visual events were synchronized with NIRSport over
400 wireless LAN communication through the Python version of LabStreamingLayer
401 (https://github.com/sccn/labstreaminglayer).
402 *Recordings in adult participants-* Experiment 1 for adults (exp1) aimed to understand
403 whether a reliable hemodynamic signal could be recorded in response to the radial
404 checkerboard merged with an animated cartoon. Thus, exp1 started with a 10-
405 minutes recording using the reversing checkerboard as stimulus 'on' and the grey
406 screen as stimulus 'off' (RS condition), and continued with the vision of two different
407 blended animated cartoons, where the stimulus 'on' was a merge between the
408 reversing checkerboard and the movie, whereas the stimulus 'off' was the grey-scale
409 isoluminant cartoon (CF and CC conditions; Fig. S1). The merging procedure was
410 achieved using Python3 OpenCV [99]. During the appearance of the stimulus each

bioRxiv preprint doi: https://doi.org/10.1101/2021.07.19.452678; this version posted July 19, 2021. The copyright holder for this preprint (which was not certified by peer review) is the author/funder, who has granted bioRxiv a license to display the preprint in perpetuity. It is made available under aCC-BY 4.0 International license.

frame was filtered using an automatic Canny edge detection algorithm (https://www.pyimagesearch.com/2015/04/06/zero-parameter-automatic-canny-edge-detection-with-python-and-opencv/), then the filtered cartoon was blended with the radial checkerboard. Each pixel of the animated cartoon with the same color of the corresponding pixel of the radial checkerboard was inverted, to obtain a fully visible image. The result was a RS with an overlayed cartoon frame (Fig 1B). The first cartoon was randomly selected by the operator within a group of 4 ("The Lion King", "The Powerpuff Girls", "Peppa Pig" or "Kung Fu Panda"; CF), whereas the latter was a free choice of the subject (CC). Exp2, aiming to dissect the contribution of baseline contrast to visual responses, was performed in a subset of adult participants (n = 15). Exp2 consisted of 3 consecutive recordings of a CF ("Peppa Pig"; "Hide-and-seek", "Fly the kite", "Polly parrot" episodes) with the modulation of the baseline contrast (20%, 40%, 80%; Fig. S1). The presentation order of different contrast levels was randomly shuffled.

Recordings in children- To confirm that the baseline movie and its contrast do not affect the emergence of visual responses to the radial checkerboard in children, we measured hemodynamic signals in response to 2 different blended RS-animated cartoons freely decided by the subject: cartoon 1 was presented at both low (20%, L1) and high (80%, H1) contrast, while only low contrast was recorded for cartoon 2 (L2; Fig. S1). In this case, the presentation order was decided by the child, in order to maximize subject compliance.

During the experimental sessions, data were quickly analyzed and visualized using nirsLAB software (NIRx Medical Technologies LLC, v2019.4).

Signal Processing and Statistical analysis

Data preprocessing was completed using the Homer3 package (v1.29.8) in MATLAB (R2020a). We created a processing stream tailored on recent guidelines for analysis of fNIRS data[22]. First, the raw intensity data were converted to optical density (OD) changes (*hmR_Intensity2OD*). Then, channels showing very high or low optical intensity were excluded from further analyses using the function *hmR_PruneChannels* (dRange: 5e-04-1e+00, SNRthresh: 2; SDrange: 0.0-45.0). Motion artifacts were then removed by a multistep rejection protocol. After a step of motion artifact detection using the *hmR_MotionArtifactByChannel* function (tMotion: 1.0, tMask: 1.0; STDEVthresh 13.0; AMPthresh: 0.40), motion correction was

bioRxiv preprint doi: https://doi.org/10.1101/2021.07.19.452678; this version posted July 19, 2021. The copyright holder for this preprint (which was not certified by peer review) is the author/funder, who has granted bioRxiv a license to display the preprint in perpetuity. It is made available under aCC-BY 4.0 International license.

performed with a combination of Spline interpolation (*hmR_MotionCorrectSpline*, p: 0.99) and Wavelet filtering (*hmR_MotionCorrectWavelet*, iqr: 0.80) functions[22]. The remaining uncorrected motion artifacts were identified using the *hmR_MotionArtifactByChannel*. A band-pass filter (*hmR_BandpassFilt: Bandpass_Filter_OpticalDensity*, hpf: 0.01, lpf: 0.50) was applied to decrease slow drifts and high-frequency noise, and the OD data were converted to Hb concentration changes using the modified Beer–Lambert law (*hmR_OD2Conc*, ppf: 1.0 1.0 1.0). Finally, trials of each subject were block-averaged for every stimulating condition and channel (*hmR_BlockAvg: Block_Average_on_Concentration_Data*, trange: -2.0 20.0)[22]. The resulting txt file was imported in Python as a Pandas DataFrame. For each subject, only the channel with the highest response amplitude was analyzed. The peak response was identified as the maximal value for THb and OHb and the minimum value for DHb. A grand average was taken of the 20 trials of data per stimulating condition and differences between visual stimulation 'on' (reversing checkerboard) and 'off' (blank) were compared. All data were normalised with respect to the blank-evoked response using a subtraction method. Statistical analysis was carried out using *pingouin* Python library [100] and the following functions: *pingouin.ttest* (paired and two-sided t-test), *pingouin.rm_anova* (one-way repeated measures ANOVA), *pingouin.pairwise_ttests* (post-hoc analysis), *pingouin.pairwise_corr* (Spearman correlation), *pingouin.regplot* (Linear regression). T-test, ANOVA and post-hoc analysis were used to assess differences in fNIRS peak responses following different stimulating conditions, whereas we tested the interaction between the amplitude of fNIRS measures and AQ scores with Spearman correlation and we employed the Linear regression to plot such correlation. Adjustments for multiple comparisons were performed using the Benjamini/Hochberg false discovery rate (BH-FDR) correction. The effect size calculated for the ANOVA was the generalized eta-squared. All the plots have been generated using *Matplotlib* Python library [101]. All statistical metrics and details are reported in Table S1.

Data availability

The datasets generated during the current study and scripts used for visual stimulation are available, respectively on Zenodo (http://doi.org/10.5281/zenodo.5101912) and GitHub website (https://github.com/raffaelemazziotti/FNIRS_code).

bioRxiv preprint doi: https://doi.org/10.1101/2021.07.19.452678; this version posted July 19, 2021. The copyright holder for this preprint (which was not certified by peer review) is the author/funder, who has granted bioRxiv a license to display the preprint in perpetuity. It is made available under aCC-BY 4.0 International license.

References

1. Maenner, M. J. *et al.* Potential impact of DSM-5 criteria on autism spectrum disorder prevalence estimates. *JAMA Psychiatry* **71**, 292–300 (2014).
2. Wing, L. The Continuum of Autistic Characteristics. *Diagnosis and Assessment in Autism* 91–110 (1988) doi:10.1007/978-1-4899-0792-9_7.
3. Posserud, M.-B., Lundervold, A. J. & Gillberg, C. Autistic features in a total population of 7-9-year-old children assessed by the ASSQ (Autism Spectrum Screening Questionnaire). *J. Child Psychol. Psychiatry* **47**, 167–175 (2006).
4. Ruzich, E. *et al.* Measuring autistic traits in the general population: a systematic review of the Autism-Spectrum Quotient (AQ) in a nonclinical population sample of 6,900 typical adult males and females. *Mol. Autism* **6**, 2 (2015).
5. Persico, A. M. & Bourgeron, T. Searching for ways out of the autism maze: genetic, epigenetic and environmental clues. *Trends Neurosci.* **29**, 349–358 (2006).
6. Ruzich, E. *et al.* Subgrouping siblings of people with autism: Identifying the broader autism phenotype. *Autism Res.* **9**, 658–665 (2016).
7. Piven, J., Palmer, P., Jacobi, D., Childress, D. & Arndt, S. Broader autism phenotype: evidence from a family history study of multiple-incidence autism families. *Am. J. Psychiatry* **154**, 185–190 (1997).
8. Billeci, L. *et al.* The Broad Autism (Endo)Phenotype: Neurostructural and Neurofunctional Correlates in Parents of Individuals with Autism Spectrum Disorders. *Front. Neurosci.* **10**, 346 (2016).
9. Carpita, B. *et al.* The broad autism phenotype in real-life: clinical and functional correlates of autism spectrum symptoms and rumination among parents of patients with autism spectrum disorder. *CNS Spectr.* **25**, 765–773 (2020).
10. Bralten, J. *et al.* Autism spectrum disorders and autistic traits share genetics and biology. *Mol. Psychiatry* **23**, 1205–1212 (2018).
11. Pagnozzi, A. M., Conti, E., Calderoni, S., Fripp, J. & Rose, S. E. A systematic review of structural MRI biomarkers in autism spectrum disorder: A machine learning perspective. *Int. J. Dev. Neurosci.* **71**, 68–82 (2018).
12. Frye, R. E. *et al.* Emerging biomarkers in autism spectrum disorder: a systematic review. *Ann Transl Med* **7**, 792 (2019).

bioRxiv preprint doi: https://doi.org/10.1101/2021.07.19.452678; this version posted July 19, 2021. The copyright holder for this preprint (which was not certified by peer review) is the author/funder, who has granted bioRxiv a license to display the preprint in perpetuity. It is made available under aCC-BY 4.0 International license.

13. Amaral, D. G., Schumann, C. M. & Nordahl, C. W. Neuroanatomy of autism. *Trends Neurosci.* **31**, 137–145 (2008).
14. Bellani, M., Calderoni, S., Muratori, F. & Brambilla, P. Brain anatomy of autism spectrum disorders I. Focus on corpus callosum. *Epidemiol. Psychiatr. Sci.* **22**, 217–221 (2013).
15. Bellani, M., Calderoni, S., Muratori, F. & Brambilla, P. Brain anatomy of autism spectrum disorders II. Focus on amygdala. *Epidemiol. Psychiatr. Sci.* **22**, 309–312 (2013).
16. Billeci, L. *et al.* On the application of quantitative EEG for characterizing autistic brain: a systematic review. *Front. Hum. Neurosci.* **7**, 442 (2013).
17. Calderoni, S., Bellani, M., Hardan, A. Y., Muratori, F. & Brambilla, P. Basal ganglia and restricted and repetitive behaviours in Autism Spectrum Disorders: current status and future perspectives. *Epidemiol. Psychiatr. Sci.* **23**, 235–238 (2014).
18. Lloyd-Fox, S., Blasi, A. & Elwell, C. E. Illuminating the developing brain: the past, present and future of functional near infrared spectroscopy. *Neurosci. Biobehav. Rev.* **34**, 269–284 (2010).
19. Gervain, J. *et al.* Near-infrared spectroscopy: a report from the McDonnell infant methodology consortium. *Dev. Cogn. Neurosci.* **1**, 22–46 (2011).
20. Raichle, M. E. & Mintun, M. A. Brain work and brain imaging. *Annu. Rev. Neurosci.* **29**, 449–476 (2006).
21. Vanderwert, R. E. & Nelson, C. A. The use of near-infrared spectroscopy in the study of typical and atypical development. *Neuroimage* **85 Pt 1**, 264–271 (2014).
22. Di Lorenzo, R. *et al.* Recommendations for motion correction of infant fNIRS data applicable to multiple data sets and acquisition systems. *Neuroimage* **200**, 511–527 (2019).
23. Yamasaki, T. *et al.* Rapid maturation of voice and linguistic processing systems in preschool children: a near-infrared spectroscopic study. *Exp. Neurol.* **250**, 313–320 (2013).
24. Mazzoni, A., Grove, R., Eapen, V., Lenroot, R. K. & Bruggemann, J. The promise of functional near-infrared spectroscopy in autism research: What do we know and where do we go? *Soc. Neurosci.* **14**, 505–518 (2019).
25. Zhang, F. & Roeyers, H. Exploring brain functions in autism spectrum disorder: A systematic review on functional near-infrared spectroscopy (fNIRS) studies.

bioRxiv preprint doi: https://doi.org/10.1101/2021.07.19.452678; this version posted July 19, 2021. The copyright holder for this preprint (which was not certified by peer review) is the author/funder, who has granted bioRxiv a license to display the preprint in perpetuity. It is made available under aCC-BY 4.0 International license.

Int. J. Psychophysiol. **137**, 41–53 (2019).

26. Keehn, B., Wagner, J. B., Tager-Flusberg, H. & Nelson, C. A. Functional connectivity in the first year of life in infants at-risk for autism: a preliminary near-infrared spectroscopy study. *Front. Hum. Neurosci.* **7**, 444 (2013).
27. Zhu, H., Fan, Y., Guo, H., Huang, D. & He, S. Reduced interhemispheric functional connectivity of children with autism spectrum disorder: evidence from functional near infrared spectroscopy studies. *Biomed. Opt. Express* **5**, 1262–1274 (2014).
28. Li, J. *et al.* Characterization of autism spectrum disorder with spontaneous hemodynamic activity. *Biomed. Opt. Express* **7**, 3871–3881 (2016).
29. Li, Y. & Yu, D. Weak network efficiency in young children with Autism Spectrum Disorder: Evidence from a functional near-infrared spectroscopy study. *Brain and Cognition* vol. 108 47–55 (2016).
30. Jia, H., Li, Y. & Yu, D. Attenuation of long-range temporal correlations of neuronal oscillations in young children with autism spectrum disorder. *Neuroimage Clin* **20**, 424–432 (2018).
31. Cao, W. *et al.* The Development of Brain Network in Males with Autism Spectrum Disorders from Childhood to Adolescence: Evidence from fNIRS Study. *Brain Sci* **11**, (2021).
32. Xu, M., Minagawa, Y., Kumazaki, H., Okada, K.-I. & Naoi, N. Prefrontal Responses to Odors in Individuals With Autism Spectrum Disorders: Functional NIRS Measurement Combined With a Fragrance Pulse Ejection System. *Front. Hum. Neurosci.* **14**, 523456 (2020).
33. Xiao, T. *et al.* Response inhibition impairment in high functioning autism and attention deficit hyperactivity disorder: evidence from near-infrared spectroscopy data. *PLoS One* **7**, e46569 (2012).
34. Lloyd-Fox, S. *et al.* Reduced neural sensitivity to social stimuli in infants at risk for autism. *Proc. Biol. Sci.* **280**, 20123026 (2013).
35. Braukmann, R. *et al.* Diminished socially selective neural processing in 5-month-old infants at high familial risk of autism. *Eur. J. Neurosci.* **47**, 720–728 (2018).
36. Lloyd-Fox, S. *et al.* Cortical responses before 6 months of life associate with later autism. *Eur. J. Neurosci.* **47**, 736–749 (2018).
37. Bhat, A. N., McDonald, N. M., Eilbott, J. E. & Pelphrey, K. A. Exploring cortical activation and connectivity in infants with and without familial risk for autism

bioRxiv preprint doi: https://doi.org/10.1101/2021.07.19.452678; this version posted July 19, 2021. The copyright holder for this preprint (which was not certified by peer review) is the author/funder, who has granted bioRxiv a license to display the preprint in perpetuity. It is made available under aCC-BY 4.0 International license.

during naturalistic social interactions: A preliminary study. *Infant Behav. Dev.* **57**, 101337 (2019).

38. Iwanaga, R. *et al.* Usefulness of near-infrared spectroscopy to detect brain dysfunction in children with autism spectrum disorder when inferring the mental state of others. *Psychiatry Clin. Neurosci.* **67**, 203–209 (2013).
39. Zhu, B. & Godavarty, A. Functional connectivity in the brain in joint attention skills using near infrared spectroscopy and imaging. *Behav. Brain Res.* **250**, 28–31 (2013).
40. Zhu, H. *et al.* Atypical prefrontal cortical responses to joint/non-joint attention in children with autism spectrum disorder (ASD): A functional near-infrared spectroscopy study. *Biomed. Opt. Express* **6**, 690–701 (2015).
41. Tamura, R., Kitamura, H., Endo, T., Abe, R. & Someya, T. Decreased leftward bias of prefrontal activity in autism spectrum disorder revealed by functional near-infrared spectroscopy. *Psychiatry Res.* **203**, 237–240 (2012).
42. Su, W.-C. *et al.* Differences in cortical activation patterns during action observation, action execution, and interpersonal synchrony between children with or without autism spectrum disorder (ASD): An fNIRS pilot study. *PLoS One* **15**, e0240301 (2020).
43. Kita, Y. *et al.* Self-face recognition in children with autism spectrum disorders: a near-infrared spectroscopy study. *Brain Dev.* **33**, 494–503 (2011).
44. Nakadoi, Y. *et al.* Multi-channel near-infrared spectroscopy shows reduced activation in the prefrontal cortex during facial expression processing in pervasive developmental disorder. *Psychiatry Clin. Neurosci.* **66**, 26–33 (2012).
45. Fox, S. E., Wagner, J. B., Shrock, C. L., Tager-Flusberg, H. & Nelson, C. A. Neural processing of facial identity and emotion in infants at high-risk for autism spectrum disorders. *Front. Hum. Neurosci.* **7**, 89 (2013).
46. Mori, K. *et al.* Neuroimaging in autism spectrum disorders: 1H-MRS and NIRS study. *J. Med. Invest.* **62**, 29–36 (2015).
47. Minagawa-Kawai, Y. *et al.* Cerebral laterality for phonemic and prosodic cue decoding in children with autism. *Neuroreport* **20**, 1219–1224 (2009).
48. Funabiki, Y., Murai, T. & Toichi, M. Cortical activation during attention to sound in autism spectrum disorders. *Res. Dev. Disabil.* **33**, 518–524 (2012).
49. Edwards, L. A., Wagner, J. B., Tager-Flusberg, H. & Nelson, C. A. Differences in Neural Correlates of Speech Perception in 3 Month Olds at High and Low Risk

bioRxiv preprint doi: https://doi.org/10.1101/2021.07.19.452678; this version posted July 19, 2021. The copyright holder for this preprint (which was not certified by peer review) is the author/funder, who has granted bioRxiv a license to display the preprint in perpetuity. It is made available under aCC-BY 4.0 International license.

for Autism Spectrum Disorder. *J. Autism Dev. Disord.* **47**, 3125–3138 (2017).

50. Pecukonis, M., Perdue, K. L., Wong, J., Tager-Flusberg, H. & Nelson, C. A. Exploring the relation between brain response to speech at 6-months and language outcomes at 24-months in infants at high and low risk for autism spectrum disorder: A preliminary functional near-infrared spectroscopy study. *Dev. Cogn. Neurosci.* **47**, 100897 (2021).
51. Yasumura, A. *et al.* Age-related differences in frontal lobe function in children with ADHD. *Brain Dev.* **41**, 577–586 (2019).
52. Chou, P.-H., Huang, C.-J. & Sun, C.-W. The Potential Role of Functional Near-Infrared Spectroscopy as Clinical Biomarkers in Schizophrenia. *Curr. Pharm. Des.* **26**, 201–217 (2020).
53. Husain, S. F. *et al.* Validating a functional near-infrared spectroscopy diagnostic paradigm for Major Depressive Disorder. *Sci. Rep.* **10**, 9740 (2020).
54. Xu, L. *et al.* Characterizing autism spectrum disorder by deep learning spontaneous brain activity from functional near-infrared spectroscopy. *J. Neurosci. Methods* **331**, 108538 (2020).
55. Yang, D., Hong, K.-S., Yoo, S.-H. & Kim, C.-S. Evaluation of Neural Degeneration Biomarkers in the Prefrontal Cortex for Early Identification of Patients With Mild Cognitive Impairment: An fNIRS Study. *Front. Hum. Neurosci.* **13**, 317 (2019).
56. Yanagisawa, K., Nakamura, N., Tsunashima, H. & Narita, N. Proposal of auxiliary diagnosis index for autism spectrum disorder using near-infrared spectroscopy. *Neurophotonics* **3**, 031413 (2016).
57. Xu, L. *et al.* Identification of autism spectrum disorder based on short-term spontaneous hemodynamic fluctuations using deep learning in a multi-layer neural network. *Clin. Neurophysiol.* **132**, 457–468 (2021).
58. Durand, S. *et al.* NMDA receptor regulation prevents regression of visual cortical function in the absence of Mecp2. *Neuron* **76**, 1078–1090 (2012).
59. de Freitas Dotto, P. *et al.* Sweep visually evoked potentials and visual findings in children with West syndrome. *Eur. J. Paediatr. Neurol.* **18**, 201–210 (2014).
60. Begenisic, T., Sansevero, G., Baroncelli, L., Cioni, G. & Sale, A. Early environmental therapy rescues brain development in a mouse model of Down syndrome. *Neurobiol. Dis.* **82**, 409–419 (2015).
61. Boggio, E. M. *et al.* Visual impairment in FOXG1-mutated individuals and mice.

bioRxiv preprint doi: https://doi.org/10.1101/2021.07.19.452678; this version posted July 19, 2021. The copyright holder for this preprint (which was not certified by peer review) is the author/funder, who has granted bioRxiv a license to display the preprint in perpetuity. It is made available under aCC-BY 4.0 International license.

Neuroscience **324**, 496–508 (2016).

62. Mazziotti, R. *et al.* Searching for biomarkers of CDKL5 disorder: early-onset visual impairment in CDKL5 mutant mice. *Hum. Mol. Genet.* **26**, 2290–2298 (2017).
63. Mazziotti, R. *et al.* Novel translational phenotypes and biomarkers for creatine transporter deficiency. *Brain Commun* **2**, fcaa089 (2020).
64. LeBlanc, J. J. *et al.* Visual evoked potentials detect cortical processing deficits in Rett syndrome. *Ann. Neurol.* **78**, 775–786 (2015).
65. Keehn, B., Westerfield, M. & Townsend, J. Brief Report: Cross-Modal Capture: Preliminary Evidence of Inefficient Filtering in Children with Autism Spectrum Disorder. *J. Autism Dev. Disord.* **49**, 385–390 (2019).
66. Little, J.-A. Vision in children with autism spectrum disorder: a critical review. *Clin. Exp. Optom.* **101**, 504–513 (2018).
67. Seymour, R. A., Rippon, G., Gooding-Williams, G., Schoffelen, J. M. & Kessler, K. Dysregulated oscillatory connectivity in the visual system in autism spectrum disorder. *Brain* **142**, 3294–3305 (2019).
68. Baron-Cohen, S., Wheelwright, S., Skinner, R., Martin, J. & Clubley, E. The autism-spectrum quotient (AQ): evidence from Asperger syndrome/high-functioning autism, males and females, scientists and mathematicians. *J. Autism Dev. Disord.* **31**, 5–17 (2001).
69. Auyeung, B., Baron-Cohen, S., Wheelwright, S. & Allison, C. The Autism Spectrum Quotient: Children's Version (AQ-Child). *J. Autism Dev. Disord.* **38**, 1230–1240 (2008).
70. Tachtsidis, I. & Scholkmann, F. False positives and false negatives in functional near-infrared spectroscopy: issues, challenges, and the way forward. *Neurophotonics* **3**, 031405 (2016).
71. Chen, L.-C., Sandmann, P., Thorne, J. D., Herrmann, C. S. & Debener, S. Association of Concurrent fNIRS and EEG Signatures in Response to Auditory and Visual Stimuli. *Brain Topogr.* **28**, 710–725 (2015).
72. Ward, L. M., Aitchison, R. T., Tawse, M., Simmers, A. J. & Shahani, U. Reduced Haemodynamic Response in the Ageing Visual Cortex Measured by Absolute fNIRS. *PLoS One* **10**, e0125012 (2015).
73. Simmons, D. R. *et al.* Vision in autism spectrum disorders. *Vision Res.* **49**, 2705–2739 (2009).

bioRxiv preprint doi: https://doi.org/10.1101/2021.07.19.452678; this version posted July 19, 2021. The copyright holder for this preprint (which was not certified by peer review) is the author/funder, who has granted bioRxiv a license to display the preprint in perpetuity. It is made available under aCC-BY 4.0 International license.

682 74. Park, W. J., Schauder, K. B., Zhang, R., Bennetto, L. & Tadin, D. High internal
683 noise and poor external noise filtering characterize perception in autism
684 spectrum disorder. *Sci. Rep.* **7**, 17584 (2017).
685 75. Noel, J.-P., Lakshminarasimhan, K. J., Park, H. & Angelaki, D. E. Increased
686 variability but intact integration during visual navigation in Autism Spectrum
687 Disorder. *Proc. Natl. Acad. Sci. U. S. A.* **117**, 11158–11166 (2020).
688 76. Noel, J.-P., Zhang, L.-Q., Stocker, A. A. & Angelaki, D. E. Individuals with autism
689 spectrum disorder have altered visual encoding capacity. *PLoS Biol.* **19**,
690 e3001215 (2021).
691 77. Turi, M., Burr, D. C. & Binda, P. Pupillometry reveals perceptual differences that
692 are tightly linked to autistic traits in typical adults. *Elife* **7**, (2018).
693 78. Tortelli, C., Turi, M., Burr, D. C. & Binda, P. Objective pupillometry shows that
694 perceptual styles covary with autistic-like personality traits. *Elife* **10**, (2021).
695 79. Hallen, R. V. der *et al.* Global processing takes time: A meta-analysis on local–
696 global visual processing in ASD. *Psychological Bulletin* vol. 141 549–573 (2015).
697 80. Ouellette, J. *et al.* Vascular contributions to 16p11.2 deletion autism syndrome
698 modeled in mice. *Nat. Neurosci.* **23**, 1090–1101 (2020).
699 81. Kozberg, M. & Hillman, E. Neurovascular coupling and energy metabolism in the
700 developing brain. *Prog. Brain Res.* **225**, 213–242 (2016).
701 82. Broadbent, J., Galic, I. & Stokes, M. A. Validation of Autism Spectrum Quotient
702 Adult Version in an Australian Sample. *Autism Research and Treatment* vol.
703 2013 1–7 (2013).
704 83. Lundqvist, L.-O. & Lindner, H. Is the Autism-Spectrum Quotient a Valid Measure
705 of Traits Associated with the Autism Spectrum? A Rasch Validation in Adults
706 with and Without Autism Spectrum Disorders. *J. Autism Dev. Disord.* **47**, 2080–
707 2091 (2017).
708 84. Wouters, S. G. M. & Spek, A. A. The use of the Autism-spectrum Quotient in
709 differentiating high-functioning adults with autism, adults with schizophrenia and
710 a neurotypical adult control group. *Research in Autism Spectrum Disorders* vol.
711 5 1169–1175 (2011).
712 85. Leekam, S. R., Nieto, C., Libby, S. J., Wing, L. & Gould, J. Describing the
713 sensory abnormalities of children and adults with autism. *J. Autism Dev. Disord.*
714 **37**, 894–910 (2007).
715 86. Scharre, J. E. & Creedon, M. P. Assessment of visual function in autistic

bioRxiv preprint doi: https://doi.org/10.1101/2021.07.19.452678; this version posted July 19, 2021. The copyright holder for this preprint (which was not certified by peer review) is the author/funder, who has granted bioRxiv a license to display the preprint in perpetuity. It is made available under aCC-BY 4.0 International license.

716 children. *Optom. Vis. Sci.* **69**, 433–439 (1992).
717 87. Apicella, F., Costanzo, V. & Purpura, G. Are early visual behavior impairments
718 involved in the onset of autism spectrum disorders? Insights for early diagnosis
719 and intervention. *European Journal of Pediatrics* vol. 179 225–234 (2020).
720 88. Kern, J. K. *et al.* Sensory correlations in autism. *Autism* vol. 11 123–134 (2007).
721 89. Jones, W. & Klin, A. Attention to eyes is present but in decline in 2-6-month-old
722 infants later diagnosed with autism. *Nature* **504**, 427–431 (2013).
723 90. McPartland, J. C. *et al.* Looking Back at the Next 40 Years of ASD Neuroscience
724 Research. *J. Autism Dev. Disord.* (2021) doi:10.1007/s10803-021-05095-5.
725 91. Baird, G., Cass, H. & Slonims, V. Diagnosis of autism. *BMJ* **327**, 488–493
726 (2003).
727 92. Zwaigenbaum, L. *et al.* Stability of diagnostic assessment for autism spectrum
728 disorder between 18 and 36 months in a high-risk cohort. *Autism Res.* **9**, 790–
729 800 (2016).
730 93. Emerson, R. W. *et al.* Functional neuroimaging of high-risk 6-month-old infants
731 predicts a diagnosis of autism at 24 months of age. *Sci. Transl. Med.* **9**, (2017).
732 94. Hazlett, H. C. *et al.* Early brain development in infants at high risk for autism
733 spectrum disorder. *Nature* **542**, 348–351 (2017).
734 95. Ruta, L., Mazzone, D., Mazzone, L., Wheelwright, S. & Baron-Cohen, S. The
735 Autism-Spectrum Quotient--Italian version: a cross-cultural confirmation of the
736 broader autism phenotype. *J. Autism Dev. Disord.* **42**, 625–633 (2012).
737 96. Vrana, A., Meier, M. L., Hotz-Boendermaker, S., Humphreys, B. K. &
738 Scholkmann, F. Cortical Sensorimotor Processing of Painful Pressure in Patients
739 with Chronic Lower Back Pain-An Optical Neuroimaging Study using fNIRS.
740 *Front. Hum. Neurosci.* **10**, 578 (2016).
741 97. Zimeo Morais, G. A., Balardin, J. B. & Sato, J. R. fNIRS Optodes' Location
742 Decider (fOLD): a toolbox for probe arrangement guided by brain regions-of-
743 interest. *Sci. Rep.* **8**, 3341 (2018).
744 98. Peirce, J. *et al.* PsychoPy2: Experiments in behavior made easy. *Behav. Res.*
745 *Methods* **51**, 195–203 (2019).
746 99. Gollapudi, S. OpenCV with Python. *Learn Computer Vision Using OpenCV* 31–
747 50 (2019) doi:10.1007/978-1-4842-4261-2_2.
748 100. Vallat, R. Pingouin: statistics in Python. *Journal of Open Source Software* vol.
749 3 1026 (2018).

bioRxiv preprint doi: https://doi.org/10.1101/2021.07.19.452678; this version posted July 19, 2021. The copyright holder for this preprint (which was not certified by peer review) is the author/funder, who has granted bioRxiv a license to display the preprint in perpetuity. It is made available under aCC-BY 4.0 International license.

101. Hunter, J. D. Matplotlib: A 2D Graphics Environment. *Computing in Science & Engineering* vol. 9 90–95 (2007).

Acknowledgements: This work was supported by a Telethon grant from GP19177 to LB, and a grant from University of Pisa (PRA-2020-50) to RB.

Author contribution: RB, GC and LB conceived the study. RM, ES, EC, VM, RR and LB designed the experiments. RM, ES and LB carried out the research. RM, ES and LB analyzed the data. LB wrote the manuscript. All authors were involved in the revision of the draft manuscript and have agreed to the final content.

Conflict of Interest: The authors declare no competing financial interests.

Figure legends

Fig.1: Visual stimulation and experimental paradigm. A: Representative frame of baseline grey screen (upper row, stimulus 'off') and reversing checkerboard (lower row, stimulus 'on') for RS condition. The small black square indicates the fixation point. **B:** Representative frame of low-contrast (20%) grey-scale baseline animated cartoon (upper row, stimulus 'off') and blended checkerboard-cartoon (lower row, stimulus 'on') for CF and CC conditions. **C:** Representative HDR in the occipital cortex during the stimulus 'off' (upper row) and stimulus 'on' activation phase (lower row) according to the output of nirsLAB software. The Look Up table is reported under the images. **D:** Experimental protocol showing that the cycles of visual stimulation were structured in blocks of 40 trials (20 trials with the reversing checkerboard and 20 trials with the 'mock' stimulus) for a total duration of 10 minutes.

Fig. 2: **HDR was reliably detected in adults using both RS and blended RS-animated cartoons.** For all panels, values in the y-axis are multiplied for 10^4. **A:** On the left, the average time course for THb (green line), OHb (red line) and DHb (blue line) in response to the RS are shown. The three plots on the right depict the

bioRxiv preprint doi: https://doi.org/10.1101/2021.07.19.452678; this version posted July 19, 2021. The copyright holder for this preprint (which was not certified by peer review) is the author/funder, who has granted bioRxiv a license to display the preprint in perpetuity. It is made available under aCC-BY 4.0 International license.

783 average peak response to the stimulus (S) vs. the blank (B) across all the adult
784 subjects. The stimulus-driven signal was significantly different from the blank for all
785 the conditions (t-test, $p < 0.001$ for all comparisons). **B:** Same plots as above for the
786 CF condition. On the left, the average time course of the evoked HDR is depicted.
787 On the right, the graphs showed that the HDR amplitude was significantly higher in
788 response to S with respect to B for THb, OHb and DHb (t-test, $p < 0.001$ for all
789 comparisons). **C:** CC condition. Also in this case the S elicited significantly higher
790 responses for THb, OHb and DHb with respect to the B (t-test, $p < 0.001$ for all
791 comparisons). **D:** Comparison among different visual stimulations (RS: Radial
792 Stimulus, CF: fixed cartoon, CC: chosen cartoon) shows no differences in evoked
793 amplitudes for THb, whereas a significant difference was detected between RS and
794 CC for OHb (One-way RM ANOVA, $p < 0.01$, post hoc BH-FDR, RS vs. CC $p < 0.01$)
795 and a more complex pattern of differences emerged for DHb (One-way RM ANOVA,
796 $p < 0.001$, post hoc BH-FDR, RS vs. CF $p < 0.01$, RS vs. CC $p< 0.001$, CF vs CC p
797 < 0.05). **E:** No differences of evoked responses were detected with different contrast
798 levels of the baseline movie (L: low, M: medium, H: high). For statistical metrics and
799 details, refer to table S1. Data are shown as average ± s.e.m. * $p < 0.05$; ** $p < 0.01$;
800 *** $p < 0.001$.
801
802 **Fig. 3**: **HDR signal was reliably detected in children using blended RS-animated**
803 **cartoons with low and high contrast.** For all panels, values in the y-axis are
804 multiplied for 10^4. **A:** On the left, the average time course for THb (green line), OHb
805 (red line) and DHb (blue line) in response to low-contrast (20%) blended RS-
806 animated cartoons is shown. On the right, the graphs represent the average
807 amplitude of the evoked HDR following the stimulus (S) and the blank (B). A
808 significantly different response to S with respect to the B was detectable for all
809 metrics (t-test, $p < 0.001$ for all comparisons). **B:** The average time course of the
810 HDR to high-contrast (80%) blended RS-animated cartoons is shown. Here, the
811 baseline cartoon is the same as the experiment described in panel A, but a different
812 part of the movie was used. THb, OHb and DHb showed a significantly higher
813 deflection to the S with respect to the B in this condition as well (t-test, $p < 0.001$ for
814 all comparisons). **C:** On the left, the average time course of HDR following the
815 second low-contrast blended RS-animated cartoon selected by the subject. On the
816 right, the analysis of peak amplitudes revealed significantly higher responses during

bioRxiv preprint doi: https://doi.org/10.1101/2021.07.19.452678; this version posted July 19, 2021. The copyright holder for this preprint (which was not certified by peer review) is the author/funder, who has granted bioRxiv a license to display the preprint in perpetuity. It is made available under aCC-BY 4.0 International license.

S compared to B for THb, OHb and DHb (t-test, $p < 0.001$ for all comparisons). **D:** Comparison among different contrast levels of the baseline cartoon revealed no differences in the amplitude of HDR. **E:** Response amplitudes for low-contrast blended RS-animated cartoons in adults and children. More specifically, we compared the response to CF condition of adults with L1 condition for children. The average amplitude of HDR was significantly higher in children (t-test, $p < 0.001$ for THb, $p < 0.05$ for OHb, $p < 0.01$ for DHb). For statistical metrics and details, refer to table S1. Data are shown as average ± s.e.m. * $p < 0.05$; ** $p < 0.01$; *** $p < 0.001$.

Fig. 4: **Correlation between HDR and AQ scores.** For all panels, values in the x-axis are multiplied for 10^4. The ρ (rho) index in each plot indicates the Spearman correlation value. **A-C:** Correlation between HDR and AQ scores in adults, for amplitudes obtained using RS (**A**), CF (**B**), and CC (**C**). No significant correlations were detected for adult participants. **D-E:** Correlation between HDR and AQ scores in children, for amplitudes obtained using high (**D**), and low (**E**) contrast baseline cartoons. A significant correlation was found between THb and AQ scores for both high- and low-contrast blended stimuli ($p < 0.05$ for both cases). Circles are individual values, lines represent the linear regression model fit and shaded regions are the 95% CI.

Fig. 5: **Correlation between HDR and AQ subscales in children.** For all panels, values in the x-axis are multiplied for x10^4. The ρ (rho) index in each plot indicates the Spearman correlation value. **A-B:** Correlations between HDR and AQ Social Skills (AQ_S) subscale. A significant correlation between THb and AQ_S was detected using both high- (A) and low-contrast blended stimuli (B; $p < 0.05$ for both cases). In addition, OHb recorded in response to the low-contrast blended RS-cartoon was significantly correlated with AQ_S (B; $p < 0.05$). **C-D:** Correlations between HDR and AQ Communication (AQ_C) subscale. THb amplitude in response to the high-contrast blended RS-cartoon was significantly correlated with AQ_C ($p < 0.05$). Circles are individual values, lines represent the linear regression model fit and shaded regions are the 95% CI.

Table 1: Demographic characteristics of adult subjects. Age (years), gender, head circumference (head, cm), cap size (cm), total AQ score (AQ), AQ subscale scores

bioRxiv preprint doi: https://doi.org/10.1101/2021.07.19.452678; this version posted July 19, 2021. The copyright holder for this preprint (which was not certified by peer review) is the author/funder, who has granted bioRxiv a license to display the preprint in perpetuity. It is made available under aCC-BY 4.0 International license.

(AQ_S, AQ_C, AQ_A, AQ_D, AQ_I) and the movies used for visual stimulation (CF and CC according to the experimental protocol) are listed for each participant. For movies, production company, release date and episode title are indicated as well.

Table 2: Demographic characteristics of children. Age (years), gender, head circumference (head, cm), cap size (cm), total AQ score (AQ), AQ subscale scores (AQ_S, AQ_C, AQ_A, AQ_D, AQ_I) and the movies used for visual stimulation (C1 and C2 according to the experimental protocol) are listed for each participant. For movies, production company, release date and episode title are indicated as well.

Fig 1

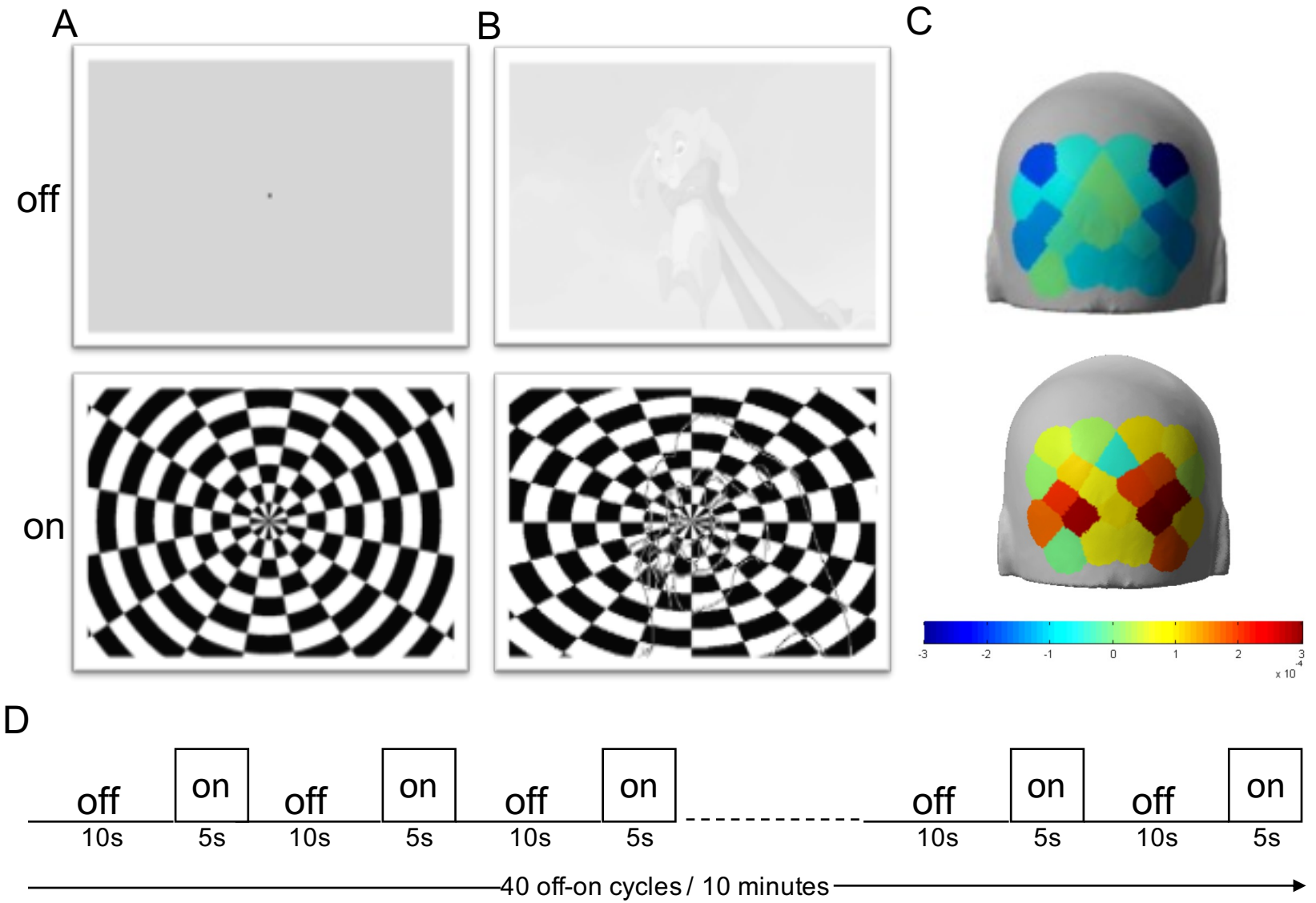
A
B
C
off
on
-3
-2
-1
0
1
2
3
x 10^-4
D
off
10s
on
5s
off
10s
on
5s
off
10s
on
5s
off
10s
on
5s
off
10s
on
5s
40 off-on cycles / 10 minutes

Fig 2

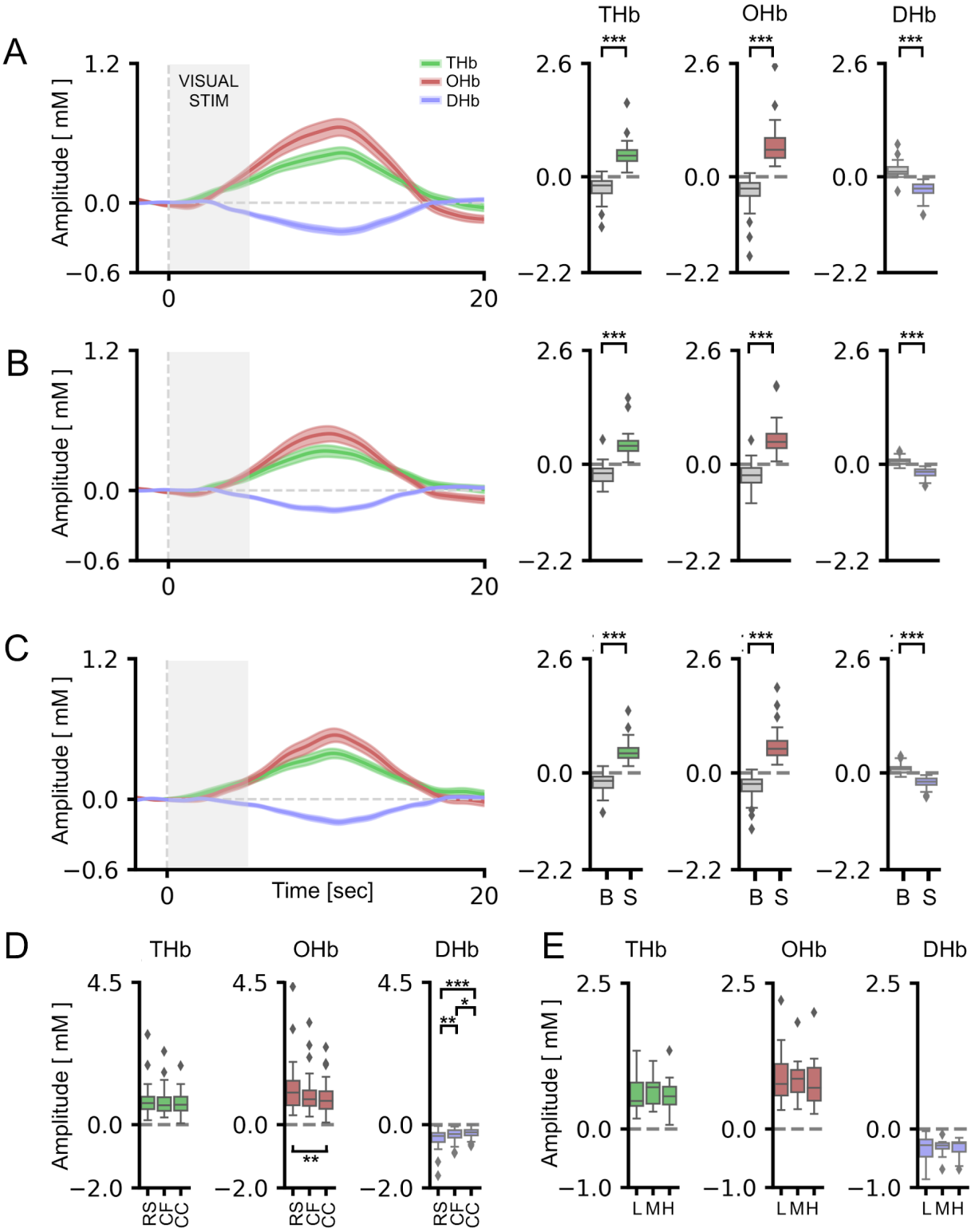
A
B
C
D
E
VISUAL STIM
THb
OHb
DHb
Amplitude [mM]
Time [sec]
B S
RS CF CC
L MH

Fig 3

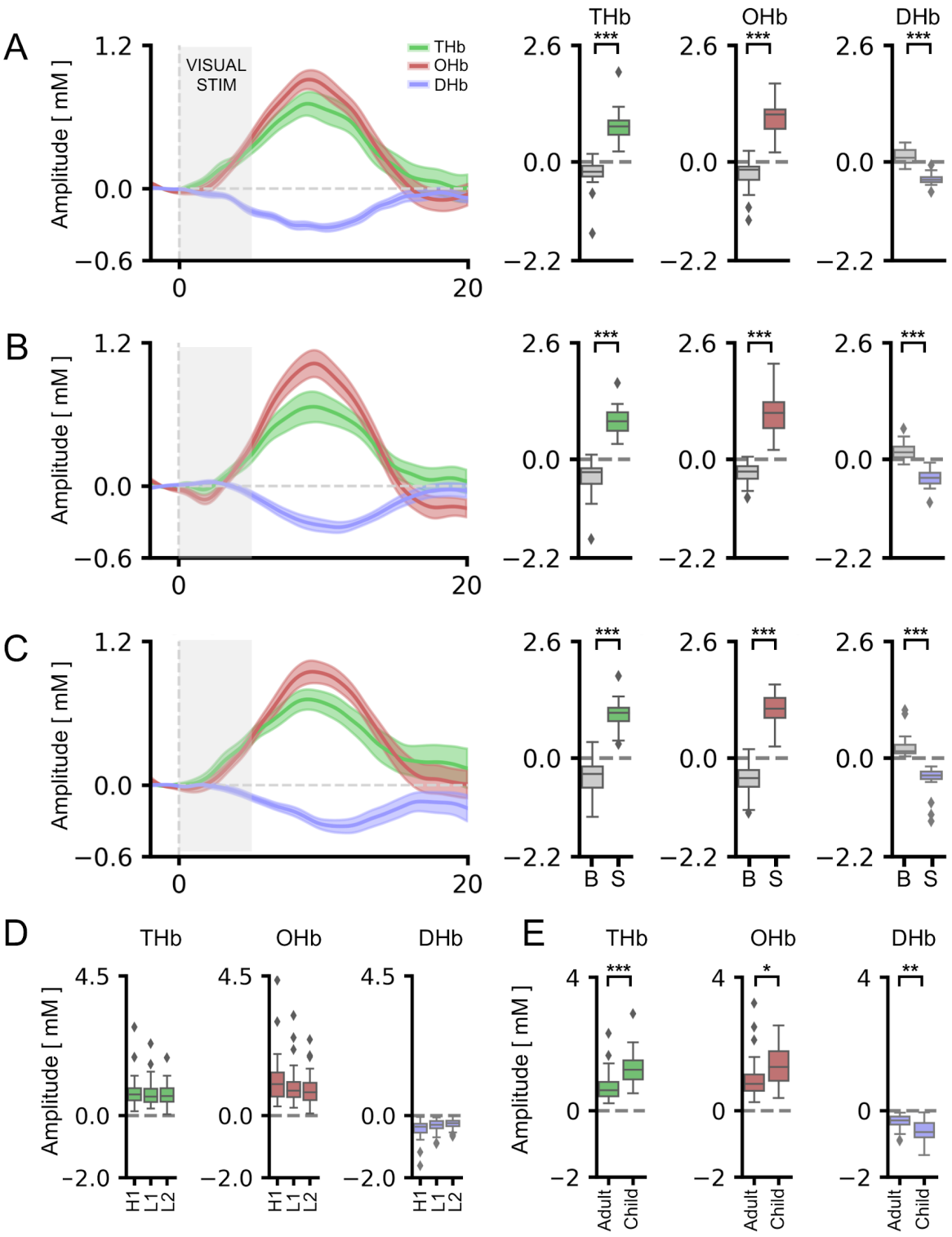
A
B
C
D
E
VISUAL STIM
THb
OHb
DHb
Amplitude [mM]
1.2
0.0
−0.6
0
20
2.6
−2.2
***
B
S
4.5
−2.0
H1
L1
L2
4
−2
*
**
Adult
Child

Fig 4

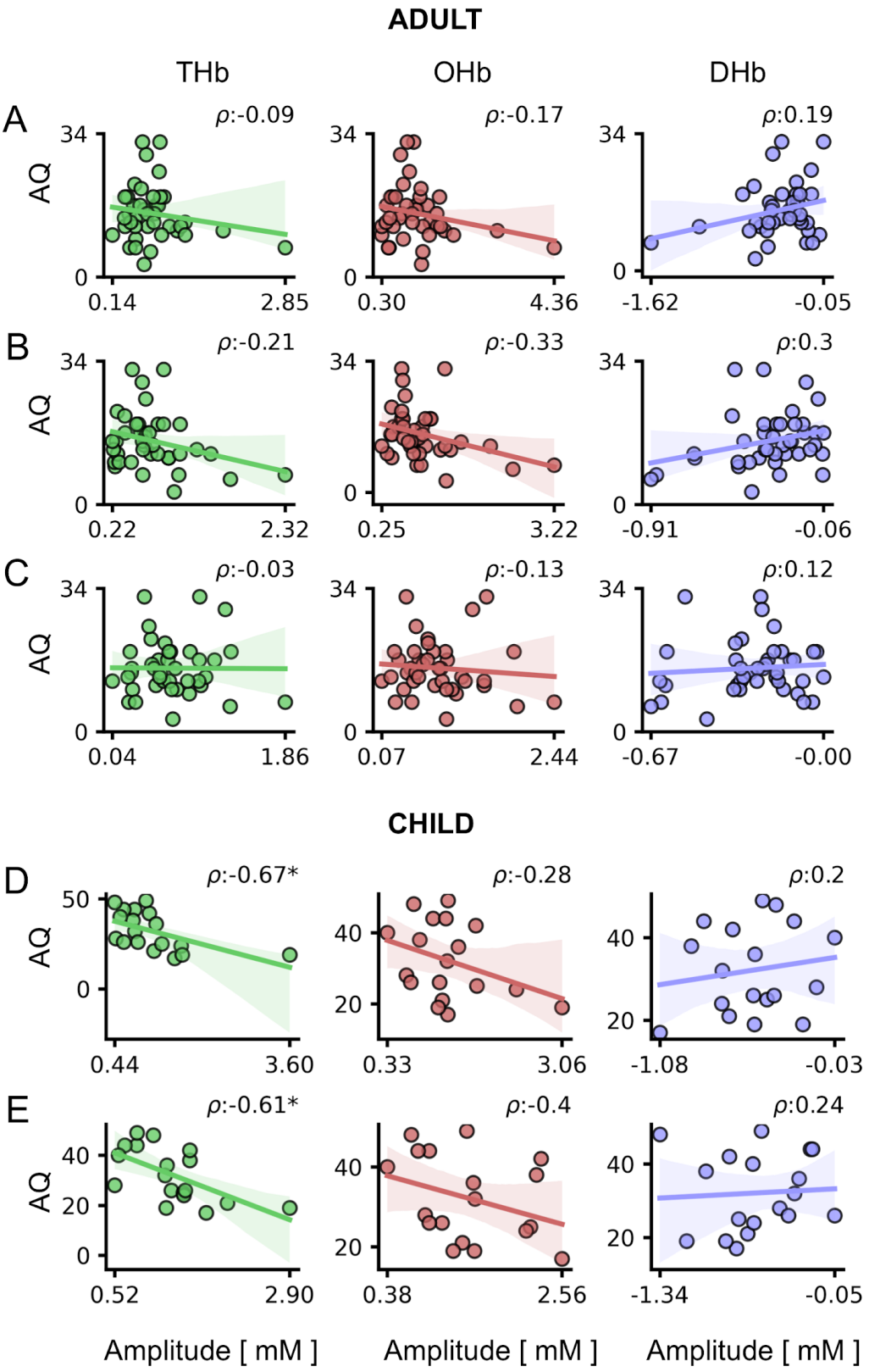
ADULT
THb
OHb
DHb
A
B
C
AQ
ρ:-0.09
ρ:-0.17
ρ:0.19
ρ:-0.21
ρ:-0.33
ρ:0.3
ρ:-0.03
ρ:-0.13
ρ:0.12
34
0
0.14
2.85
0.30
4.36
-1.62
-0.05
0.22
2.32
0.25
3.22
-0.91
-0.06
0.04
1.86
0.07
2.44
-0.67
-0.00
CHILD
D
E
ρ:-0.67*
ρ:-0.28
ρ:0.2
ρ:-0.61*
ρ:-0.4
ρ:0.24
50
40
20
0.44
3.60
0.33
3.06
-1.08
-0.03
0.52
2.90
0.38
2.56
-1.34
-0.05
Amplitude [mM]
Amplitude [mM]
Amplitude [mM]

Fig 5

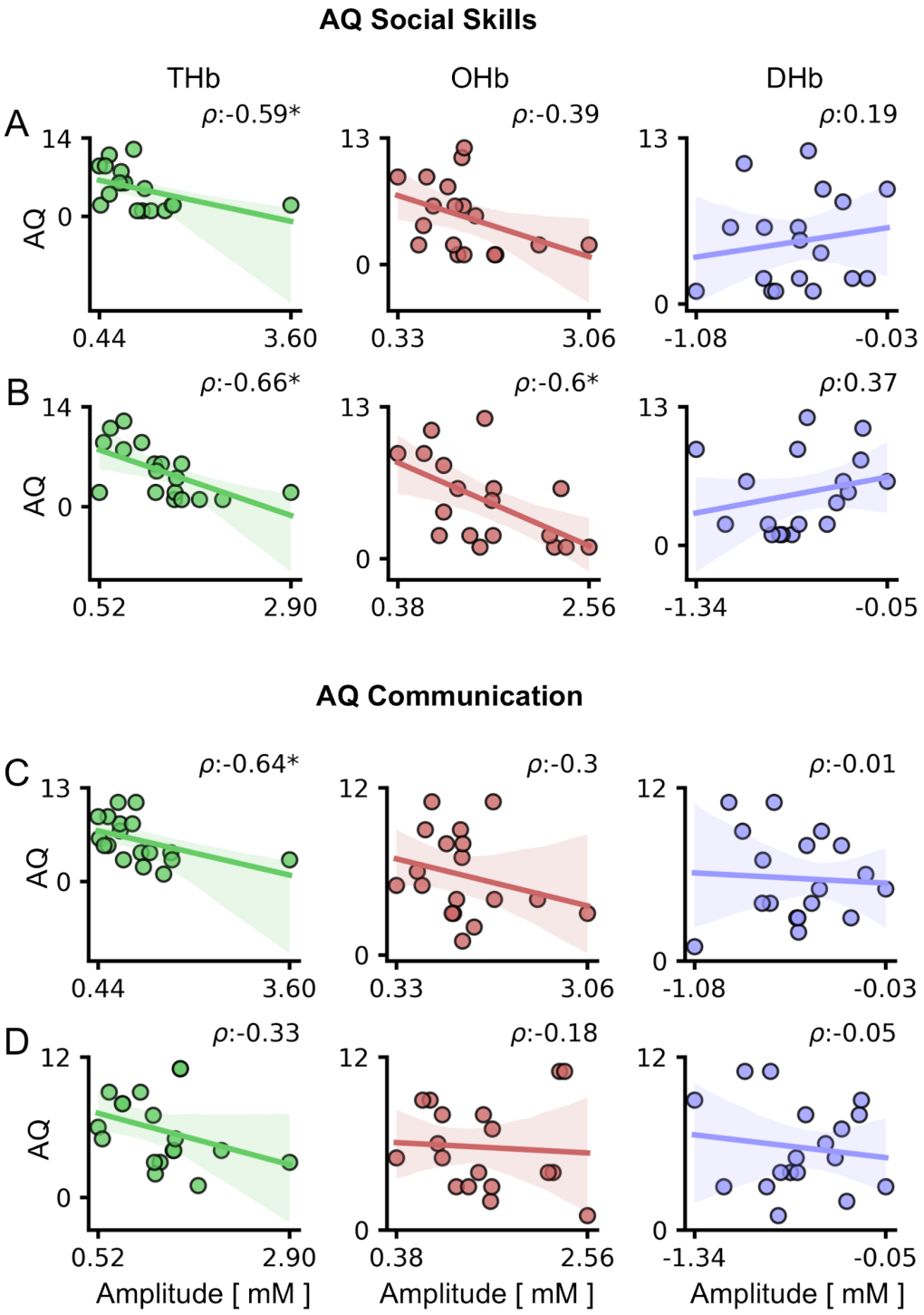
AQ Social Skills
THb
OHb
DHb
A
ρ:-0.59*
ρ:-0.39
ρ:0.19
AQ
14
0
13
0
13
0
0.44
3.60
0.33
3.06
-1.08
-0.03
B
ρ:-0.66*
ρ:-0.6*
ρ:0.37
14
0
13
0
13
0
0.52
2.90
0.38
2.56
-1.34
-0.05
AQ Communication
C
ρ:-0.64*
ρ:-0.3
ρ:-0.01
13
0
12
0
12
0
0.44
3.60
0.33
3.06
-1.08
-0.03
D
ρ:-0.33
ρ:-0.18
ρ:-0.05
12
0
12
0
12
0
0.52
2.90
0.38
2.56
-1.34
-0.05
Amplitude [mM]
Amplitude [mM]
Amplitude [mM]

ID	Age	Gender	Head	Cap size	AQ	AQ_S	AQ_C	AQ_A	AQ_D	AQ_I	CF	CC
A1	29	F	57	56	11	0	1	7	1	2	The Lion King Walt Disney Pictures,1994	The Sword in the Stone Walt Disney Productions,1963
A2	36	F	56	56	17	0	0	6	9	2	The Powerpuff Girls special episode "Twas the Fight Before Christmas", Cartoon Network Studios, 2003	The Aristocats Walt Disney Productions,1970
A3	35	M	57	56	17	3	3	5	0	6	Kung Fu Panda DreamWorks Animation, 2008	Aladdin Walt Disney Pictures,1992
A4	28	F	57	56	3	0	0	1	1	1	Peppa Pig “Hide-and-seek”, “Fly the kite”, “Polly parrot” episodes, Entertainment One, 2004	The Simpsons S29E02 “Springfield Splendor”, 20th Television, 2017
A5	25	F	57	56	19	4	1	7	6	1	The Lion King Walt Disney Pictures,1994	101 Dalmatians Walt Disney Productions,1961
A6	35	F	57	56	15	4	2	4	5	0	The Powerpuff Girls special episode "Twas the Fight Before Christmas", Cartoon Network Studios, 2003	The Simpsons S29E02 “Springfield Splendor”, 20th Television, 2017
A7	29	F	57	56	11	0	2	5	3	1	Peppa Pig “Hide-and-seek”, “Fly the kite”, “Polly parrot” episodes, Entertainment One, 2004	101 Dalmatians Walt Disney Productions,1961
A8	30	F	56	56	13	0	2	4	5	2	Kung Fu Panda DreamWorks Animation, 2008	Wall-E Disney-Pixar, 2008
A9	29	F	59	56	7	1	1	3	2	0	The Lion King Walt Disney Pictures,1994	The Sword in the Stone Walt Disney Productions,1963
A10	29	M	58	56	12	1	1	5	4	1	The Powerpuff Girls special episode "Twas the Fight Before Christmas", Cartoon Network Studios, 2003	Aladdin Walt Disney Pictures,1992
A11	27	M	56.5	56	17	2	3	5	4	3	Peppa Pig “Hide-and-seek”, “Fly the kite”, “Polly parrot” episodes, Entertainment One, 2004	101 Dalmatians Walt Disney Productions,1961
A12	30	F	56	56	9	1	2	2	3	1	Kung Fu Panda DreamWorks Animation, 2008	Inside out Disney-Pixar, 2015
A13	29	M	57	56	14	1	3	6	2	2	The Lion King Walt Disney Pictures,1994	Wall-E Disney-Pixar, 2008
A14	36	M	58.5	56	19	2	2	5	7	3	The Powerpuff Girls special episode "Twas the Fight Before Christmas", Cartoon Network Studios, 2003	101 Dalmatians Walt Disney Productions,1961
A15	36	M	57	56	16	4	1	4	5	2	Peppa Pig “Hide-and-seek”, “Fly the kite”, “Polly parrot” episodes, Entertainment One, 2004	Aladdin Walt Disney Pictures,1992
A16	29	F	54	56	22	1	3	9	7	2	Kung Fu Panda DreamWorks Animation, 2008	The Rescuers Walt Disney Productions,1977
A17	28	F	58.5	56	7	1	0	2	1	3	The Lion King Walt Disney Pictures,1994	101 Dalmatians Walt Disney Productions,1961
A18	29	F	55	56	12	0	1	5	5	1	The Powerpuff Girls special episode "Twas the Fight Before Christmas", Cartoon Network Studios, 2003	Peter Pan Walt Disney Productions,1953
A19	34	M	60	56	19	6	2	5	5	1	Peppa Pig “Hide-and-seek”, “Fly the kite”, “Polly parrot” episodes, Entertainment One, 2004	SpongeBob S12E01 “FarmerBob”, Nickelodeon Animation Studio, 2018
A20	26	M	58	56	10	3	0	5	2	0	Kung Fu Panda DreamWorks Animation, 2008	Inside out Disney-Pixar, 2015

A21	36	F	56	56	15	1	2	2	7	3	The Lion King Walt Disney Pictures,1994	Inside out Disney-Pixar, 2015
A22	30	M	60.5	56	19	1	2	6	4	6	The Lion King Walt Disney Pictures,1994	The Sword in the Stone Walt Disney Productions,1963
A23	26	F	56	56	12	0	1	5	6	0	The Powerpuff Girls special episode "Twas the Fight Before Christmas", Cartoon Network Studios, 2003	Wall-E Disney-Pixar, 2008
A24	32	M	60.5	56	7	0	1	5	0	1	Kung Fu Panda DreamWorks Animation, 2008	Aladdin Walt Disney Pictures,1992
A25	34	F	56	56	10	1	1	4	2	2	The Lion King Walt Disney Pictures1994	Beauty and the Beast Walt Disney Pictures,1994
A26	29	F	57	56	32	6	5	8	9	4	The Powerpuff Girls special episode "Twas the Fight Before Christmas", Cartoon Network Studios, 2003	The Aristocats Walt Disney Productions,1970
A27	31	M	59	56	32	10	6	6	2	8	Kung Fu Panda DreamWorks Animation, 2008	The Simpsons S29E02 “Springfield Splendor”, 20th Television, 2017
A28	39	F	57	56	21	2	4	4	8	3	Peppa Pig “Hide-and-seek”, “Fly the kite”, “Polly parrot” episodes, Entertainment One, 2004	Lady Oscar, “A Funeral Bell Tolls in the Twilight" episode, Discotek Media, 1980
A29	29	M	57	56	6	0	0	2	2	2	The Lion King Walt Disney Pictures,1994	The Simpsons S29E02 “Springfield Splendor”, 20th Television, 2017
A30	29	M	57	56	17	3	2	5	6	1	The Powerpuff Girls special episode "Twas the Fight Before Christmas", Cartoon Network Studios, 2003	The Sword in the Stone Walt Disney Productions,1963
A31	36	M	59.5	56	12	0	0	6	4	2	Peppa Pig “Hide-and-seek”, “Fly the kite”, “Polly parrot” episodes, Entertainment One, 2004	The Sword in the Stone Walt Disney Productions,1963
A32	27	M	59	56	12	1	2	5	2	2	The Powerpuff Girls special episode "Twas the Fight Before Christmas", Cartoon Network Studios, 2003	The Aristocats Walt Disney Productions,1970
A33	40	M	57	56	13	2	3	1	6	1	Peppa Pig “Hide-and-seek”, “Fly the kite”, “Polly parrot” episodes, Entertainment One, 2004	The Simpsons S29E02 “Springfield Splendor”, 20th Television, 2017
A34	31	F	55	56	15	1	1	4	4	5	Kung Fu Panda DreamWorks Animation, 2008	The Sword in the Stone Walt Disney Productions,1963
A35	27	M	56.5	56	19	6	2	4	7	0	The Lion King Walt Disney Pictures,1994	Frozen Walt Disney Pictures, 2013
A36	30	M	58	56	14	5	1	3	4	1	The Powerpuff Girls special episode "Twas the Fight Before Christmas", Cartoon Network Studios, 2003	Wall-E Disney-Pixar, 2008
A37	25	M	58	56	29	6	8	6	7	2	Peppa Pig “Hide-and-seek”, “Fly the kite”, “Polly parrot” episodes, Entertainment One, 2004	Wall-E Disney-Pixar, 2008
A38	31	M	57.5	56	10	0	1	5	3	1	Kung Fu Panda DreamWorks Animation, 2008	Inside out Disney-Pixar, 2015
A39	38	M	57.5	56	25	2	4	6	8	5	The Lion King Walt Disney Pictures,1994	The Sword in the Stone Walt Disney Productions,1963
A40	33	F	57.5	56	13	0	0	3	10	0	The Powerpuff Girls special episode "Twas the Fight Before Christmas", Cartoon Network Studios, 2003	Beauty and the Beast Walt Disney Pictures,1994

ID	Age	Gender	Head	Cap size	AQ	AQ-S	AQ_C	AQ_A	AQ_D	AQ_I	C1 (L1 and H1)	C2 (L2)
B1	5	M	51.5	52	21	1	4	7	5	4	Uncle Grandpa S3E04 "Uncle Easter", Cartoon Network Studios, 2016	Teen Titans Go! To the Movies Warner Bros. Animation, 2018
B2	5	M	51	52	32	6	7	3	10	6	Wile E. Coyote & Road Runner “Coyote falls”, ""Fur of flying” and “Rabid rider” episodes, Acme Corporation, 2010	ABCs song Little Baby Bum - Nursery Rhymes & Kids Songs youtube channel, 2014
B3	13	M	57	56	26	6	3	4	7	6	The Simpsons S29E02 “Springfield Splendor”, 20th Television, 2017	Futurama, S7E01 “The Bots and the Bees”, Comedy Central, 2012
B4	12	M	56	56	44	8	8	11	13	4	The Incredibles Disney-Pixar, 2004	Wile E. Coyote & Road Runner “Coyote falls”, ""Fur of flying” and “Rabid rider” episodes, Acme Corporation, 2010
B5	12	M	56	56	25	1	4	10	0	10	Big Hero 6 Walt Disney Pictures, 2014	The Amazing World of Gumball S01E01 "The DVD", Cartoon Network Development Studio Europe, 2011
B6	6	F	53	52	17	1	1	4	8	3	Inside out Disney-Pixar, 2015	Floopaloo S1E22 "Squirrel for a Day", Marc du Pontavice, 2012
B7	7	M	53	52	24	2	4	1	12	5	The Chipmunks “Bye, George” episode, DIC Entertainment, 1989	Floopaloo S1E22 "Squirrel for a Day", Marc du Pontavice, 2012
B8	4	F	50.5	52	38	6	11	7	11	3	Frozen Walt Disney Pictures, 2013	Bolt Walt Disney Pictures, 2008
B9	4	M	52	52	42	1	11	11	13	6	Spider-Man: Into the Spider-Verse Columbia Pictures, 2018	Bolt Walt Disney Pictures, 2008
B10	4	M	51	52	n.a.	n.a.	n.a.	n.a.	n.a.	n.a.	Cars Walt Disney Pictures, 2006	Thomas & Friends "Diesel and the duckling" episode, Mattel, 2019
B11	9	F	54	56	28	2	6	3	13	4	The Simpsons S29E02 “Springfield Splendor”, 20th Television, 2017	Zig & Sharko S01E28 “Moby Zig”, Xilam Animation, 2010
B12	8	M	54.5	56	26	4	5	5	4	8	Beauty and the Beast Walt Disney Pictures,1994	Ice Age Blue Sky Studios, 2002
B13	4	M	53	56	44	11	9	8	9	7	Finding Nemo Disney-Pixar 2003	101 Dalmatians Walt Disney Productions,1961
B14	6	M	53	52	36	5	2	3	19	7	Trolls DreamWorks Animation, 2016	Curious George S1E03 "Zeros to Donuts", Universal Animation Studios, 2006
B15	7	M	51.5	52	49	12	8	10	9	10	Cars Walt Disney Pictures, 2006	Pup Academy S1E02 “Tell Us About Your Human Day”, Air Bud Entertainment, 2019
B16	10	F	55	56	48	9	9	10	10	10	Frozen Walt Disney Pictures, 2013	Descendants Disney Channel Original Productions, 2015
B17	10	M	54	56	40	9	5	7	13	6	The Simpsons S29E02 “Springfield Splendor”, 20th Television, 2017	Uncle Grandpa S3E04 "Uncle Easter", Cartoon Network Studios, 2016
B18	4	F	49.5	52	19	2	3	5	6	3	Frozen Walt Disney Pictures, 2013	Bing S1E06 “Smoothie”, Tandem Films e Digitales Studios, 2014
B19	7	M	54	56	19	2	3	5	6	3	Ranger Rob S1E12 "Big Stink in Big Sky Park" Nelvana Enterprises Inc, 2016	Arex&Vastatore “Casket of fear” episode Arex&Vastatore YouTube Channel, 2021